Stripe pattern formation in phase separation accompanying orientational ordering under an external field

2006 J. Phys.: Condens. Matter 18 L305

(http://iopscience.iop.org/0953-8984/18/22/L05)

INSTITUTE OF PHYSICS PUBLISHING JOURNAL OF PHYSICS: CONDENSED MATTER

J. Phys.: Condens. Matter **18** (2006) L305–L314 doi:10.1088/0953-8984/18/22/L05

LETTER TO THE EDITOR

Stripe pattern formation in phase separation accompanying orientational ordering under an external field

Takeaki Araki and Hajime Tanaka

Institute of Industrial Science, University of Tokyo, Meguro-ku, Tokyo 153-8505, Japan

Received 2 February 2006, in final form 27 April 2006
Published 19 May 2006
Online at stacks.iop.org/JPhysCM/18/L305

Abstract

We demonstrate field-induced formation of stripe domains in phase separation accompanying orientational ordering, taking a mixture of an isotropic liquid and a nematic liquid crystal as an example. We can classify spinodal decomposition, which is governed by coupling between conserved compositional and non-conserved orientational ordering, into two types: isotropic and anisotropic spinodal decomposition. In the former, phase separation occurs prior to orientational ordering. Thus, an isotropic phase-separated pattern is formed in the early stage even under an external field. In the latter, on the other hand, a homogeneous oriented phase is formed prior to phase separation under an external field. Then anisotropic domains grow by phase separation. We reveal that the kinetic pathway in the two-dimensional order parameter space is key to field-induced stripe formation. This principle may be commonly applied to a mixture, one of whose components has orientational ordering such as spin, dipolar or orbital ordering. We also confirm that the anisotropic pattern has a memory of orientation of the applied external field, which may be used for device applications.

(Some figures in this article are in colour only in the electronic version)

1. Introduction

Phase separation is often used for the formation of heterogeneous structures of various materials including metals, semiconductors, simple liquids and complex fluids such as polymers, surfactants and liquid crystals [1]. However, the morphological variety formed by phase separation is rather limited. For an isotropic system, either a bicontinuous or a droplet structure can be formed depending upon the volume fraction of a binary mixture. Viscoelastic and elastic effects sometimes lead to sponge or network morphology [1, 2]. One of the most promising ways to control phase-separation morphology is to apply an external field such as an electric [3] and a magnetic field. In this paper we study how we can produce anisotropic patterns by

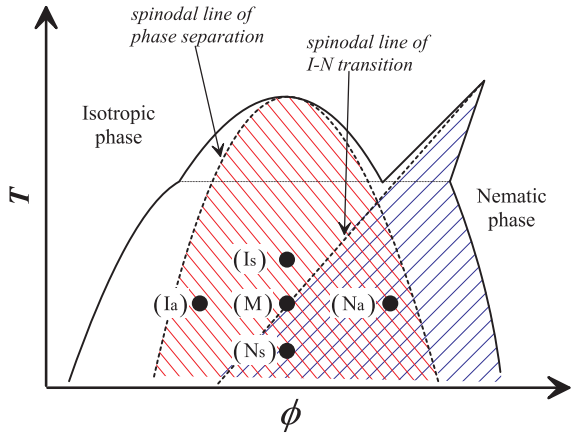

Figure 1. Schematic phase diagram of an IL–LC mixture. Points (I_a), (N_s), (I_s), (M) and (N_s) correspond to simulations (a) and (b) in figure 2, and (a)–(c) in figure 4, respectively. Suffixes 'a' and 's' denote an asymmetric (off-critical) and symmetric (critical) mixture, respectively.

applying an external field to phase separation, taking a mixture of an isotropic liquid and a liquid crystal as an explicit example.

In a mixture of an isotropic liquid (IL) and a liquid crystal (LC), both compositional (phase separation) and orientational ordering (nematic ordering) can take place simultaneously. Figure 1 shows a typical phase diagram of such a mixture, which is composed of the coexistence curve and the isotropic–nematic (I–N) transition line. This competing ordering has attracted considerable interest both technological [4] and scientific [5–19]. Theoretically the phase-separation kinetics is described by the coupled dynamics of the two order parameters, composition ϕ and orientational order parameter Q [20]. This is somewhat similar to the ordering dynamics of so-called model C [1], which for example describes the ordering of a He^3–He^4 mixture (competition between phase separation and superfluid transition) [21].

Depending upon which ordering process takes place first, two types of spinodal decomposition can occur [9, 11–13, 16, 21]. In isotropic spinodal decomposition (ISD) (at points I_a and I_s in figure 1), phase separation proceeds first and then isotropic–nematic transition follows it. In nematic spinodal decomposition (NSD) (at points N_a and N_s in figure 1), on the other hand, nematic ordering takes place first and phase separation follows it. Phase separation of an IL–LC mixture is also affected by the elasticity of the liquid crystal. In some cases, nematohydrodynamic effects also play important roles in phase separation and the resulting pattern formation [19]. Here we neglect hydrodynamic effects since we focus on the early stage of spinodal decomposition, which is dominated by diffusion, and are also interested in dynamic features of coupled order parameter dynamics common to solid systems.

This paper is organized as follows. We describe our model of phase separation in a mixture of IL and LC and our simulation method in section 2. In section 3, we show our numerical results and discuss them. We summarize our paper in section 4.

2. Model and numerical method

First, we describe a coarse-grained model of phase separation of an IL–LC mixture [19]. Here we consider only a two-dimensional (2D) system for simplicity. We employ the Landau–Ginzburg type free energy for the concentration field: $f_{\rm mix}(T,\phi) = -\frac{1}{2}\tau(T)\phi^2 + \frac{u}{4}\phi^2$, where

$\tau(T)$ is a coefficient depending on temperature T and u is a positive constant [1]. $\phi > 0$ corresponds to the LC-rich phase. To describe I–N transition, we employ the Landau–de Gennes type free energy for the orientational order: $f_{\mathrm{LdG}}(T, \phi, \boldsymbol{Q}) = \mathrm{Tr}\{-\frac{1}{2}a(T, \phi)\boldsymbol{Q}^2 - \frac{1}{3}b\boldsymbol{Q}^3 + \frac{1}{4}c\boldsymbol{Q}^4\}$ [20], where b and c are positive constants and $a(T, \phi)$ increases with decreasing T and increasing ϕ, respectively. Here the nematic ordering is treated as a second-order phase transition, i.e. $b = 0$, since it should be the case for two dimensions, which we study here. By employing proper dependences of $\tau(T)$ and $a(T, \phi)$ on temperature and composition, we obtain a phase diagram for a mixture of IL and LC as shown in figure 1. The total Ginzburg–Landau type free-energy functional of the system is given by[1]

$$\mathcal{F}\{\phi, Q_{ij}\} = k_{\mathrm{B}}T \int \mathrm{d}V \left\{ f_{\mathrm{mix}}(\phi) + \frac{K_\phi}{2}|\nabla\phi|^2 + f_{\mathrm{LdG}}(\phi, Q_{ij}) + \frac{K_Q}{2}(\partial_k Q_{ij})^2 + w\partial_i\phi\partial_j\phi Q_{ij} - \chi e_i e_j Q_{ij} \right\}. \tag{1}$$

Here K_ϕ and K_Q are the coefficients of the gradient energy for concentration and nematic order, which are related to the interface tension and the Frank elasticity, respectively. The fifth term in equation (1) represents the anchoring energy of the director field to the interface. A positive w leads the director field to be parallel along the interface, i.e. planar anchoring, which we consider here. e_i is an external field, which is coupled to the orientational order parameter $\boldsymbol{Q}$, and χ represents its susceptibility. Here we do not consider the dependence of dielectric or magnetic permeability on the concentration and thus neglect a coupling between e_i and ϕ for simplicity. k_{B} is Boltzmann's constant.

Next we describe the dynamic equations for ϕ and $\boldsymbol{Q}$:

$$\frac{\partial}{\partial t}\phi = D\nabla^2(\mu/k_{\mathrm{B}}T) + \theta, \tag{2}$$

$$\frac{\partial}{\partial t}Q_{ij} = L(H_{ij}/k_{\mathrm{B}}T) + \lambda_{ij}, \tag{3}$$

where μ and $\boldsymbol{H}$ are the chemical potential and the molecular force field, respectively; $\mu = \frac{\delta\mathcal{F}}{\delta\phi}$ and $\boldsymbol{H} = -(\frac{\delta\mathcal{F}}{\delta\boldsymbol{Q}} - \frac{1}{2}\boldsymbol{I}\,\mathrm{Tr}\frac{\delta\mathcal{F}}{\delta\boldsymbol{Q}})$. D and L represent diffusional and rotational coefficients, respectively. In equations (2) and (3), we neglect the off-diagonal Onsager coefficients between ϕ and $\boldsymbol{Q}$; they are known to be important for polymeric LC [14–18] but negligible for low-molecular-weight LC, which we consider here.

The equilibrium values of the concentration and orientational order parameter depend upon the temperature via $\tau(T)$ and $a(T, \phi)$, respectively. This leads to the changes in physical properties such as the interface tension, the Frank elastic constants and the susceptibility of the director field to the external field. In order to pick up solely a difference between ISD and NSD, here we use the fully normalized compositional and orientational order parameters. The concentration is scaled by the equilibrium one that is free from I–N transition, $\phi_{\mathrm{e}} = \sqrt{\tau(T)/u}$, and the length is scaled by the correlation length of concentration fluctuations, $\xi = \sqrt{K_\phi/\tau(T)}$. Note that we consider only the case of $\tau(T) > 0$. Then, the free energy functional can be scaled by $\sigma\xi^2$. Here σ is the interface tension defined by $\sigma = kk_{\mathrm{B}}TK_\phi\phi_{\mathrm{e}}^2/\xi$ [1], where k is a numerical factor, $k = 2^{3/2}/3$. The orientational order parameter is also scaled by the equilibrium one of the homogeneous nematic phase, whose concentration is ϕ_{e}, i.e. $Q_{\mathrm{e}} = \sqrt{a(T, \phi_{\mathrm{e}})/c}$. After the normalization, the third and fourth terms in equation (1) are rewritten as

[1] Free energy functionals of semiflexible polymer solutions were derived from the microscopic Hamiltonian [6, 7]. They generally include the following coupling terms between the concentration and orientational order parameter: $\partial_i\phi\partial_j Q_{ij}$, $\phi\boldsymbol{Q}^2$, $\partial_i\phi\partial_j\phi Q_{ij}$, $\phi^2\boldsymbol{Q}^2$ and higher-order terms. For simplicity, we retain only $\phi\boldsymbol{Q}^2$ and $\partial_i\phi\partial_j\phi Q_{ij}$, which we believe are crucial for describing the kinetics of phase separation in a mixture of low-molecular components.

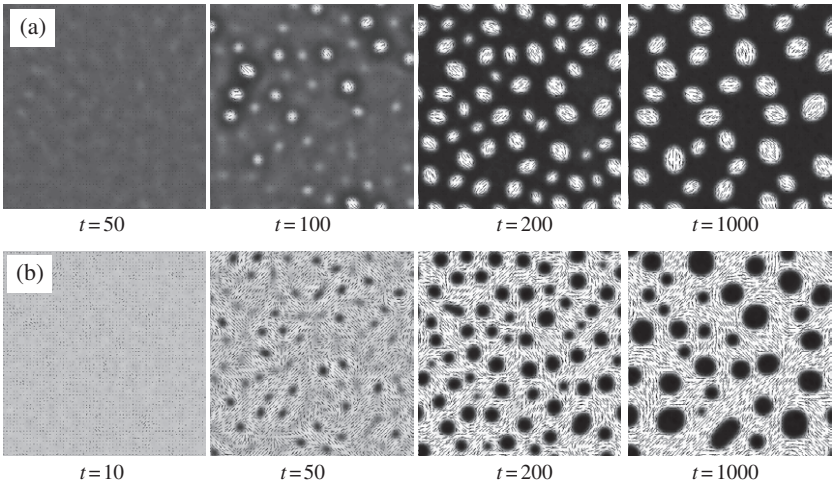

Figure 2. Simulated phase-separation processes of the IL-rich (a) and LC-rich (b) mixture. Their initial compositions are $\phi_0 = -0.5$ and 0.5, respectively, and we set $\phi^* = 0.0$. The brightness represents the concentration field ϕ and the director field is indicated by lines.

$\alpha\left\{-\frac{1}{2}a'(\phi)\boldsymbol{Q}^2 + \frac{1}{4}\boldsymbol{Q}^2 + \frac{1}{2}\epsilon^2(\partial_k Q_{ij})^2\right\}$. Hereafter $\boldsymbol{Q}$ denotes the tensorial orientational order parameter scaled by Q_e. α is the ratio between the interfacial and elastic energy; $\alpha = k\frac{K_F\xi}{\sigma\Xi^2}$, where Ξ is the correlation length of the orientational order parameter, $\Xi = \sqrt{K_Q/a(T,\phi_e)}$, and K_F is the Frank elastic modulus, $K_F = k_B T K_Q Q_e^2$. ϵ is the ratio between the two correlation lengths, $\epsilon = \Xi/\xi$. $a'(\phi)$ is an increasing function of the concentration and satisfies $a'(\phi_e) = 1$ and $a'(\phi^*) = 0$, where ϕ^* is the threshold concentration above which nematic ordering takes place. Here we assume $a'(\phi) = \frac{\phi-\phi^*}{\phi_e-\phi^*}$ as the simplest form. Note that in our model a quench condition is determined solely by ϕ_0 and ϕ^*. We also scale the coefficient of the anchoring energy as $W = \frac{wQ_e}{K_\phi}$ and normalize the external field as $E_i = \sqrt{\chi/Q_e}e_i$. In equations (2) and (3), time is scaled by the characteristic lifetime of concentration fluctuations, ξ^2/D. Therefore, $L\alpha\xi^2/D$ represents the scaled characteristic rotational relaxation rate of a phase-separated nematic phase.

We numerically solve equation (3) by using an explicit Euler scheme, in which the discretized space and time are $\Delta x = 1$ and $\Delta t = 0.01$. We set $\alpha = 0.2$, $\epsilon = 0.4$, $W = 0.2$ and $L\xi^2/D = 25$.[2] We keep imposing the Gaussian noises whose intensities are $|\theta| = 1 \times 10^{-2}$ and $|\lambda_{ij}| = 1 \times 10^{-2}$, respectively, in equations (2) and (3).

3. Results and discussion

3.1. Isotropic and nematic spinodal

First we study phase-separation kinetics of two asymmetric mixtures; the IL-rich ($\phi_0 = -0.5$) and the LC-rich mixture ($\phi_0 = 0.5$) at $\phi^* = 0.0$. These IL-rich and LC-rich mixtures just after the quench correspond to points (I_a) and (N_a) in figure 1, respectively. Figures 2(a) and (b) show the pattern evolution for mixtures (I_a) and (N_a), respectively. Since the initial composition ϕ_0 is lower than the threshold ϕ^* for mixture (I_a), it is unstable for phase separation but stable for the

[2] These values are estimated from typical values obtained experimentally: $\sigma \sim 5 \times 10^{-4}$ (N m^{-1}), $K_F \sim 5 \times 10^{-12}$ (N), $k_B T\phi_e^2 Q_e w/\xi \sim 10^{-4}$ (N m^{-1}), $\xi \sim 2.5 \times 10^{-8}$ (m) and $\Xi \sim 10^{-8}$ (m).

I–N transition. Thus, phase separation proceeds first and then nematic ordering takes place only in LC-rich regions ($\phi > \phi^*$) after $t \approx 100$, which corresponds to ISD. The volume fraction of the LC-rich phase is about 25% and thus it forms droplets. We employed the positive anchoring parameter ($W = 0.2$) in all simulations; thus, the director field tends to align parallel to the interface. Accordingly, bipolar-type nematic droplets are formed in the late stage. Because of the interface anchoring and the elastic effects, the droplet shape is elongated along the orientational field inside the droplet. The interface and anchoring energy are proportional to R^2 (R being a characteristic size of droplets), whereas the elastic one is proportional to R. Thus for small droplets the director field is not distorted inside a droplet, but the shape is largely deformed (see, for example, the pattern at $t = 100$ in figure 2(a)). For large droplets, on the other hand, the anchoring and interface energy become dominant, and thus the director field is deformed (see, for example, the pattern at $t = 1000$ of figure 2(a)).

For a mixture (N_a), whose initial concentration ϕ_0 is higher than ϕ^*, the mixture becomes unstable for both phase separation and the I–N transition. The kinetics of nematic ordering is usually faster than that of phase separation, since the orientational order parameter is non-conserved and can be changed locally. Thus, nematic ordering proceeds in the entire system, and then phase separation follows. This behaviour corresponds to NSD. In the IL-rich phase formed by phase separation, the nematic phase becomes unstable and thus is transformed back to the isotropic phase. Since these isotropic droplets are surrounded by the nematic phase, the shape of these IL-rich droplets reflects the director orientation in the nematic phase [16]. Although this effect is rather weak in figure 2(b), we confirmed that it plays a significant role for cases of larger ϵ and W. Here we note that phase separation in both mixture (I_a) and (N_a) proceeds via spinodal decomposition, not via nucleation and a growth mechanism [1]; in other words, a system is unstable against infinitesimal concentration fluctuations.

Figure 3(a) shows the two different kinetic pathways of phase separation of mixtures (I_a) and (N_a) on the ϕ–Q plane. Here, we defined the region where $\phi > 0$ as the LC-rich phase and vice versa. A difference in the kinetic pathway between ISD and NSD can be clearly seen. Figure 3(b) shows the time development of the amplitude of concentration fluctuation $I(t) = \int \mathrm{d}V(\phi(t) - \phi_0)^2$ for mixtures (I_a) and (N_a). We can see that the growth of concentration fluctuation in NSD is faster than that in ISD. Since the stability against phase separation, i.e. the distance from the spinodal line, is the same between mixtures (I_a) and (N_a), the difference in the growth rate should be due to the nematic ordering in NSD. This is explained by the enhancement of concentration fluctuation due to nematic ordering [12]. It has been reported that the off-diagonal Onsager kinetic coefficients also play an important role in the early stage of NSD [15, 17]. Since they are set to be zero in our simulations, however, the origin of the above difference is not the off-diagonal coupling between ϕ and Q_{ij}. Provided that in NSD the nematic phase is ordered before phase separation starts, we can approximate the chemical potential as $\mu \approx \left[-\tau + 3u\phi_0^2 - a''(\phi_0)\boldsymbol{Q}^2 - K_\phi\nabla^2 - 2w\partial_j(Q_{ij}\partial_i)\right]\delta\phi$, where $\delta\phi = \phi - \phi_0$ stands for concentration fluctuations. If phase separation starts from the isotropic phase, i.e. for ISD, it is well known [1] that the growth rate of concentration fluctuation is given by $\Gamma^{\mathrm{ISD}}(q) = Dq^2(1 - 3\phi_0^2/\phi_e^2 - \xi^2q^2)$ (q is the wavenumber) in our notation. Thus, the maximum growth rate is simply calculated as $\Gamma_m^{\mathrm{ISD}} = D(1 - 3\phi_0^2/\phi_e^2)^2/(4\xi^2)$ at $q = \sqrt{(1 - 3\phi_0^2/\phi_e^2)/(2\xi^2)}$. In NSD, on the other hand, the maximum growth rate depends upon the orientational field as

$$\Gamma_m^{\mathrm{NSD}}(\hat{q}) \approx \frac{D\left\{1 - 3\phi_0^2/\phi_e^2 + a''(\phi_0)\boldsymbol{Q}^2/\tau\right\}^2}{4\xi^2(1 + 2wQ_{ij}\hat{q}_i\hat{q}_j/K_\phi)}, \tag{4}$$

where $\hat{q} = \vec{q}/|\vec{q}|$ is the unit vector having the direction of the wavevector. The wavenumber giving the maximum growth rate also depends on the director field as $q_\parallel \propto (1 + w\bar{Q}/K_\phi)^{-1/2}$

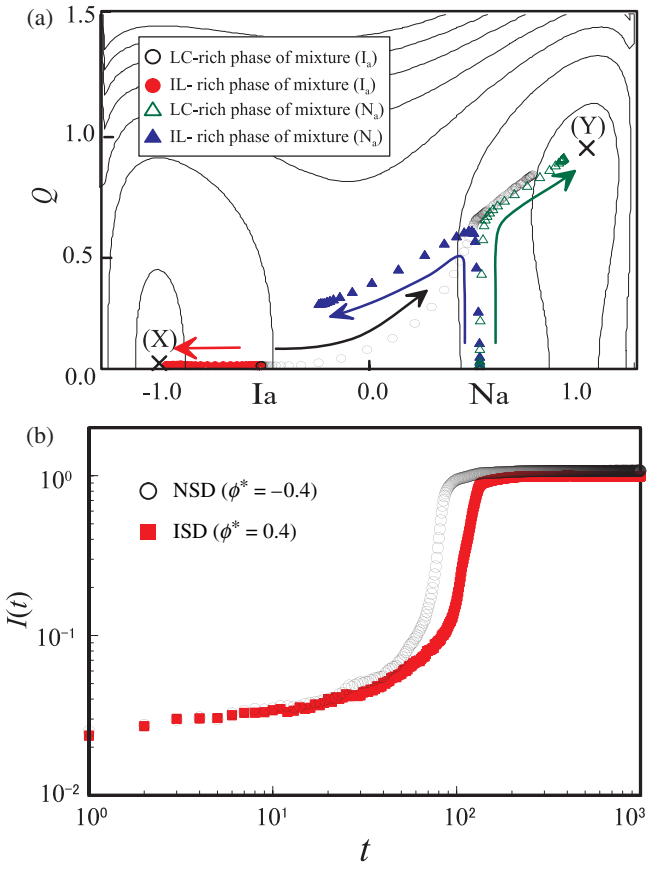

Figure 3. (a) Time development of ϕ and Q, both of which are averaged over the IL and LC-rich phase, for mixtures (I_a) and (N_a), plotted on the contour plot of the free energy $f_{\rm mix}(\phi)+f_{\rm LdG}(\phi, Q)$ of a mixture of $\phi^* = 0$. Points (X) and (Y) correspond to the equilibrium IL and LC-rich phases, respectively. (b) Time development of $I(t)$ for asymmetric mixtures (I_a) (ISD) and (N_a) (NSD).

and $q_\perp \propto (1 - w\bar{Q}/K_\phi)^{-1/2}$ for the directions parallel and perpendicular to the initial nematic phase, respectively. Here $\bar{Q}$ is the degree of the nematic order before phase separation. Since $\Gamma_{\rm m}^{\rm NSD}(\hat{q}_\parallel) < \Gamma_{\rm m}^{\rm NSD}(\hat{q}_\perp)$, a perpendicular mode of concentration fluctuation grows faster than a parallel one, which leads to anisotropic spinodal decomposition. This is consistent with the mechanism of stripe formation from a pre-oriented state [18, 22]. Since $\Gamma_{\rm m}^{\rm NSD}(\hat{q}_\perp) > \Gamma_{\rm m}^{\rm ISD}$, anisotropic spinodal decomposition proceeds faster than ISD. We believe that this faster growth rate, which stems from the tensorial nature of the nematic order parameter, plays a more important role in the early stage of NSD than the coupled growth rate given by off-diagonal kinetic coefficients.

3.2. Anisotropic domain pattern formation

Next we discuss the difference in domain pattern evolution between ISD and NSD, focusing on the effects of an external field. In order to pick up solely the difference between ISD and NSD, we performed numerical simulations of symmetric mixtures $\phi_0 = 0$. To clarify the difference, we also simulated a mixture with neutral SD ($\phi_0 \approx \phi^*$), which is just on the border of ISD and NSD. We set $\phi^* = 0.4$, 0.0 and -0.4 for ISD, neutral SD and NSD, respectively

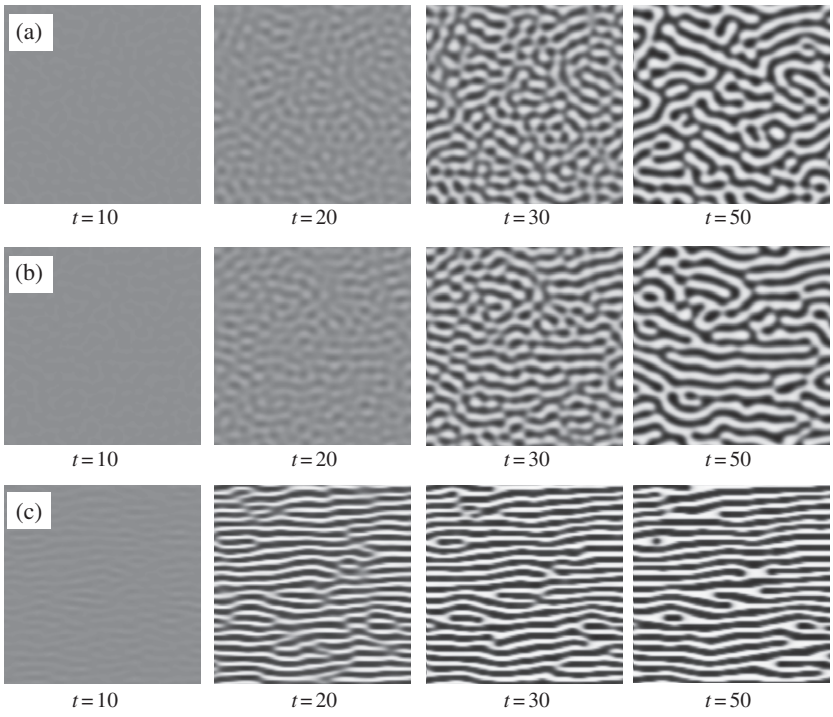

Figure 4. Simulated domain pattern evolution of symmetric mixtures under an external field. Phase separation in (a)–(c) proceeds via ISD ($\phi^* = 0.4 > \phi_0$), neutral SD ($\phi^* = \phi_0$), and NSD ($\phi^* = -0.4 < \phi_0$), respectively, which correspond to points (I_s), (M) and (N_s) in figure 1.

(see points (I_s), (M) and (N_s) in figure 1). We applied the external field $\vec{E} = (0.2, 0.0)$ to these mixtures. Figures 4(a)–(c) show the simulated pattern evolution of mixtures (I_s), (M) and (N_s), respectively. In the early stage of mixture (I_s) (see figure 4(a)), phase separation proceeds before nematic ordering, and thus the isotropic domain pattern is formed. In mixture (N_s), on the other hand, phase separation proceeds via NSD. This nematic order develops before phase separation. The director field is aligned along the external field without interference from concentration fluctuations. Thus, the anisotropic stripe domain pattern emerges from the ordered nematic phase along the external field, as observed experimentally [23]. Since the director field in the LC-rich phase tends to be parallel to the external field, the domain interface also tends to align along the field owing to the coupling between $\nabla\phi$ and Q_{ij} at the interface. Once isotropic domains are formed in the early stage as in figure 4(a), however, it is not easy to control the morphology by the external field since it takes a quite long time for domains to be deformed by an external field. As shown in figure 4(c), the application of an external field to the nematic ordering before phase separation is a very promising way to control the domain pattern. Note that we neglect a coupling between E_i and ϕ. Thus, the anisotropic pattern in figure 4(c) is not driven directly by the external field but implicitly via the growing nematic order coupled with the field. More precisely, the external field $\vec{E}$ controls the orientational field $\boldsymbol{Q}$ via $E_i E_j Q_{ij}$, and then $\boldsymbol{Q}$ affects the concentration ϕ via $W\partial_i\phi\partial_j\phi Q_{ij}$. Therefore, the external field does not affect phase separation for ISD, where $\boldsymbol{Q}$ is small (see, for example, figure 4(a)).

Figure 5(a) shows the temporal evolution of the structure factor $S(q_y)$ for figure 4(c). The scattering pattern (figure 5(b)) is strongly anisotropic as expected. $S(q_y)$ has a distinct peak

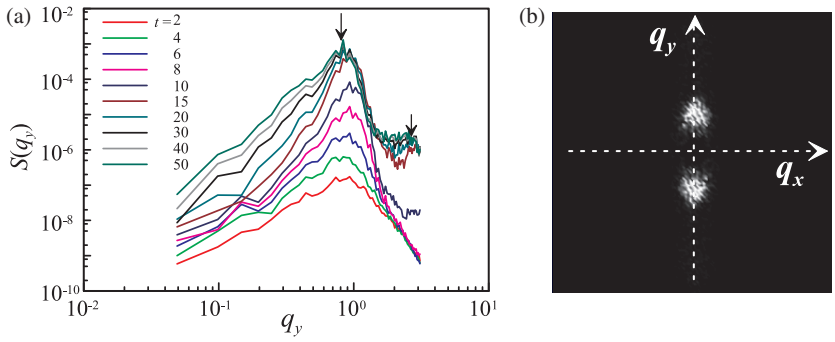

Figure 5. (a) Temporal evolution of the structure factor of symmetric spinodal decomposition via NSD (figure 4(c)) for the y-direction. The arrows indicate the first and second peaks at $q_y = q_\perp$ and $3q_\perp$, respectively. (b) The scattering pattern $S(\vec{q})$ at $t = 50$ is drawn. The structure factors correspond to the cross section of the two-dimensional scattering pattern at $q_x = 0$.

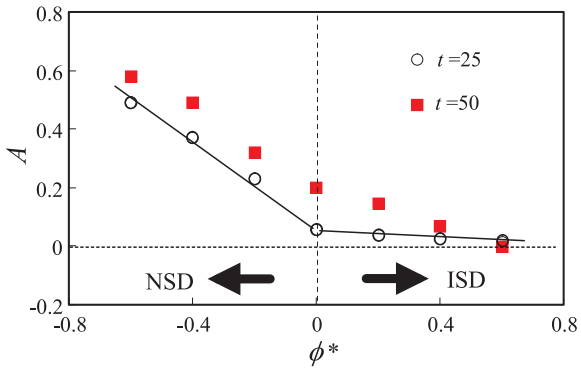

Figure 6. The dependence of the anisotropy on ϕ^* of the resulting domain pattern A under an external field.

at $q_y = q_\perp$, which is the inverse of the wavelength of the most unstable mode of spinodal decomposition. The second-order scattering peak is also observed, reflecting the sharp stripe order. This tells us that NSD under an external field can produce the stripe pattern, whose period is nearly the correlation length of concentration fluctuations, in the early stage of phase separation, with a help of the interfacial anchoring effects.

Figure 6 shows the dependence of ϕ^* on the anisotropy of the resulting domain pattern under an external field, which is the same as those in figure 4. The anisotropy is defined by $A = \int dV\{(\partial_y\phi)^2 - (\partial_x\phi)^2\}/\int dV|\nabla\phi|^2$, where x is along the external field. Note that the value of A for a completely isotropic pattern is zero. The anisotropy decreases with increasing ϕ^*, which is consistent with the results in figure 4. In the early stage ($t = 25$), the difference in the anisotropy between ISD and NSD is more remarkable and the ϕ^* dependence of A has a distinct kink at $\phi^* \approx \phi_0$. This kink becomes less significant as the time elapses. This is because the domain pattern slowly aligns along the external field to reduce the total free energy even for $\phi^* > \phi_0$. Thus, we can conclude that to attain a perfectly aligned stripe domain pattern we should initiate orientational ordering prior to phase separation under an external field.

Stripe pattern formation in IL–LC mixtures was reported for phase separation of a homogeneously oriented nematic phase [18, 22, 23]. Here we demonstrate that a highly ordered stripe pattern can be formed even from an isotropic phase for NSD under an external field.

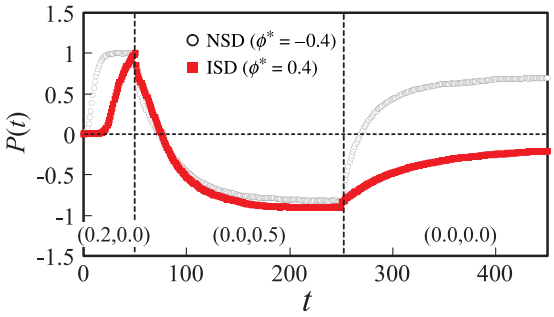

Figure 7. Temporal change of $P(t)$ for ISD ($\phi^* = 0.4$) and NSD ($\phi^* = -0.4$), which correspond to figures 4(a) and (c), respectively. We applied a horizontal external field (0.2, 0.0) for $0 < t < 50$ and then a vertical field (0.0, 0.5) for $50 < t < 250$. At $t = 250$ we switched off the applied field.

Key roles are played in this anisotropic compositional ordering by homogeneous orientational ordering prior to phase separation under the external field, which is due to faster ordering of the (non-conserved) orientational order parameter than the (conserved) compositional one, and the interfacial anchoring, which induces the coupling of the orientational order and the interface orientation.

3.3. Memory effects of anisotropic domains

Finally, we show memory effects of anisotropic domains prepared by NSD. We use two patterns in figures 4(a) and (c) at $t = 50$ as the initial patterns and study the response of the orientational order to the applied external field. Figure 7 shows the temporal change of the scaled orientational order, $P(t) = \int \mathrm{d}V\,(Q_{xx}(t) - Q_{yy}(t))/\int \mathrm{d}V\,(Q_{xx}(50) - Q_{yy}(50))$, during this process. The behaviour is essentially the same between ISD and NSD until $t = 250$. After the external field is turned off at $t = 250$, however, the difference between ISD and NSD becomes evident. For ISD, $P(t)$ gradually approaches zero, which indicates that the orientation inside nematic droplets is randomized by the thermal fluctuation. For NSD, on the other hand, it quickly recovers the orientational state at $t = 50$. This is because the elongated nematic droplets remember the original orientational field inside them via the anchoring effect of the domain interface. Thus, we can say that anisotropic droplets formed by NSD can memorize the initial configuration of the orientational field effectively. This should have relevance to applications.

4. Summary

To summarize, we propose a new physical principle for the formation of an ordered stripe pattern with orientational memory effects. This principle relies on a novel kinetic pathway of competing orderings under an external field, whose key ingredients are (i) the faster ordering of non-conserved orientational (vector or tensor) order parameters than conserved compositional (scalar) ones, (ii) the direct coupling of the orientational order to an external field and (iii) an orientation–composition gradient coupling at the interface. Although we show results for phase separation with liquid crystal ordering, we expect that the same principle may be applied to phase separation accompanying any orientational ordering including spin, dipolar and orbital ordering.

This work was partially supported by a grant-in-aid from the Ministry of Education, Culture, Sports, Science and Technology, Japan.

References

[1] Onuki A 2002 *Phase Transition Dynamics* (Cambridge: Cambridge University Press)
[2] Tanaka H 2000 *J. Phys.: Condens. Matter* **12** R207
[3] Schäuffer E, Thurn-Albrecht T, Russell T P and Steiner U 2000 *Nature* **403** 874
[4] Doane J W, Golemme A, West J L, Whitehead J B Jr and Wu B G 1988 *Mol. Cryst. Liq. Cryst.* **165** 511
[5] Palffy-Muhoray P, de Bruyn J J and Dunmur D A 1985 *Mol. Cryst. Liq. Cryst.* **127** 301
[6] Liu A and Fredrickson G H 1993 *Macromolecules* **26** 2817
[7] Fukuda J 1999 *Eur. Phys. J.* B **7** 573
[8] Holyst R and Schick M 1992 *J. Chem. Phys.* **96** 721
[9] Ten Bosch A 1991 *J. Physique* II **1** 949
[10] Shen C and Kyu T 1985 *J. Chem. Phys.* **102** 556
[11] Lansac Y, Fried F and Maïssa P 1995 *Liq. Cryst.* **18** 829
[12] Matsuyama A, Evans R M L and Cates M E 2000 *Phys. Rev.* E **61** 2977
[13] Chiu H W and Kyu T 1999 *J. Chem. Phys.* **110** 5998
[14] Shimada T, Doi M and Okano K 1988 *J. Chem. Phys.* **88** 7181
[15] Liu A J and Fredrickson G H 1993 *Macromolecules* **26** 2817
[16] Lapeña A M, Glotzer S C, Langer S A and Liu A J 1999 *Phys. Rev.* E **60** R29
[17] Fukuda J 1999 *Phys. Rev.* E **59** 3275
[18] Fukuda J 1998 *Phys. Rev.* E **58** R6939
[19] Araki T and Tanaka H 2004 *Phys. Rev. Lett.* **93** 015702
[20] de Gennes P G and Prost J 1993 *The Physics of Liquid Crystals* 2nd edn (Oxford: Clarendon)
[21] Hohenberg P C and Nelson D R 1979 *Phys. Rev.* B **20** 2665
[22] Essery R L H and Ball R C 1991 *Europhys. Lett.* **16** 379
[23] Casagrande C, Veyssie M and Knobler C M 1987 *Phys. Rev. Lett.* **58** 2079